Conformational Dynamics of the GdmHCl-Induced Molten Globule State of Creatine Kinase Monitored by Hydrogen Exchange and Mass Spectrometry

Hortense Mazon,[‡] Olivier Marcillat,[‡] Eric Forest,[§] David L. Smith,[||] and Christian Vial*[,‡]

UMR CNRS 5013, Biomembranes et enzymes associés, Université Claude Bernard Lyon I, 43, boulevard du 11 Novembre 1918, 69622 Villeurbanne Cedex, France, Laboratoire de spectrométrie de masse des protéines, Institut de Biologie Structurale, CNRS (UMR 5075)/CEA/UJF, 41, rue Jules Horowitz, 38027 Grenoble Cedex, France, and Department of Chemistry, University of Nebraska, Lincoln, Nebraska 68588-0304

Received January 5, 2004; Revised Manuscript Received February 24, 2004

ABSTRACT: Our understanding of the mechanism of protein folding can be improved by the characterization of folding intermediate states. Intrinsic tryptophan fluorescence measurements of equilibrium GdmHCl-induced unfolding of MM-CK allow for the construction of a "phase diagram", which shows the presence of five different conformational states, including three partially folded intermediates. However, only three states are detected by using pulsed-labeled H−D exchange analyzed by electrospray ionization mass spectrometry. One of them is the native state, and the two other species are present in proportions strongly dependent on the GdmHCl concentration and denaturation time. The low-mass peak is due to a largely exchange-incompetent state, which has gained only ∼10 deuteriums more than the native protein. This population of MM-CK molecules has undergone a small conformational change induced by low GdmHCl concentrations. However, this limited change is in itself not sufficient to inactivate the enzyme or is easily reversible. The high-mass peak corresponds to a population of MM-CK that is fully deuterated. The comparison of fluorescence, activity, and H−D exchange measurements shows that the maximally populated intermediate at 0.8 M GdmHCl has the characteristics of a molten globule. It has no activity; it has 55% of its native α-helices and a maximum fluorescence emission wavelength of ∼341 nm, and it binds ANS strongly. However, no protection against exchange is detected under the conditions used in this work. This paradox, the presence of significant residual secondary and tertiary structures detected by optical probes and the total deuteration of its amide protons detected by H−D exchange and mass spectrometry, could be explained by a highly dynamic MM-CK molten globule.

Protein folding is one of the most challenging subjects in structural biology, and characterization of folding−unfolding intermediates is a necessary step for the elucidation of its mechanisms. A large amount of experimental data has been acquired with small, single-domain proteins, but large, multidomain, and oligomeric proteins have been explored less. The folding−unfolding processes of these proteins are complicated by association and dissociation of subunits. Moreover, folding and oligomerization events may be linked (*1*).

For many small monomeric proteins such as lysozyme (*2*), α-lactalbumin (*3*), and ribonuclease A (*4*), an equilibrium intermediate possessing similar characteristics, defined as the molten globule state, has been detected between the native and fully unfolded states (*5*). This state is usually characterized by a relatively compact and globular shape, exposed hydrophobic areas that strongly bind the fluorescent probe ANS,[1] a prononced secondary structure, and a fluctuating tertiary structure (*3*, *6*). This state seems to be not only an equilibrium intermediate in folding−unfolding processes but also an early kinetic intermediate on the folding pathway of proteins (*6*−*9*).

Creatine kinase (CK) isoenzymes are members of the large family of phosphagen kinases. They catalyze the reversible transfer of a phosphoryl group from $MgATP^{2-}$ to creatine, generating phosphocreatine and $MgADP^{-}$ in the cells of excitable tissues (for a review, see ref *10*). The X-ray structure of several CKs has recently been determined. These include octameric mitochondrial CK from chicken heart (*11*) and from human placenta (*12*) and dimeric cytosolic CKs from rabbit, chicken, ox, and human (*13*−*16*). These structures exhibit a high degree of homology, in accordance with their high level of sequence similarity (∼60% identical across all species). They share the same subunit topology. Each monomer displays a two-domain organization with a small N-terminal domain (∼100 residues) containing only helices and a large C-terminal domain (residues 120−380) consisting of an eight-stranded antiparallel β-sheet sur-

* To whom correspondence should be addressed: UMR 5013 CNRS, Université Claude Bernard Lyon I, 43 boulevard du 11 Novembre 1918, 69622 Villeurbanne Cedex, France. Telephone: 00 33 472 448 248. Fax: 00 33 472 431 557. E-mail: christian.vial@univ-lyon1.fr.

[‡] Université Claude Bernard Lyon I.

[§] CNRS (UMR 5075)/CEA/UJF.

[||] University of Nebraska.

[1] Abbreviations: ANS, 8-anilino-1-naphthalenesulfonic acid; H−D, hydrogen−deuterium; CD, circular dichroism; DTT, dithiothreitol; EDTA, ethylenediaminetetraacetic acid; ESI-MS, electrospray ionization mass spectrometry; GdmHCl, guanidine hydrochloride; HPLC, high-performance liquid chromatography; MM-CK, cytosolic dimeric creatine kinase MM; NMR, nuclear magnetic resonance; TFA, trifluoroacetic acid; UV, ultraviolet.

10.1021/bi049965b CCC: $27.50
Published on Web 04/02/2004

rounded by seven α-helices. The active site is located in a cleft between the two domains. Sequence alignment of the CK isoenzymes reveals six highly conserved regions, which form a compact core involved in substrate binding and catalysis (*11*). Several monomer−monomer contact areas allow the formation of a stable dimer (*17*, *18*). Surface loops that are highly flexible have been observed in all known CKs around residues 59−69, 182−204, and 320−330, and they are believed to be involved in rearrangements of the structure to shield the active site from water during catalysis (*19*, *20*). A unique site of cleavage by proteinase K is located in the C-terminal loop of native CKs (*21*−*23*). Cleavage at this site inactivates the enzyme (*24*). Otherwise, native CKs are highly resistant to specific proteases, which indicates that CK has a rather compact structure (*21*, *23*, *25*). However, low denaturant concentrations enhance the susceptibility to proteases (*26*) and allow exposure of otherwise hidden epitopes (*27*). This sensitivity to denaturant results from a limited unfolding within the hydrophobic shell of the protein (*28*) and from a disruption of monomer−monomer contacts (*17*).

The folding and unfolding of CK are complex and involve several intermediates (*25*, *29*, *30*−*36*). The most abundant intermediate observed at moderate concentrations (0.6−1 M) of GdmHCl is a molten globule, but the occurrence of an inactive dimer, a compact monomer, and a pre-molten globule has also been suggested together with that of misfolded species leading to aggregate formation on the folding pathway, depending on the experimental conditions. Our aim was to better characterize the molten globule intermediate during the unfolding of a multidomain dimeric protein such as MM-CK.

Hydrogen exchange has become a powerful tool in analyzing the structure and dynamics of proteins (*37*, *38*). When a protein is incubated in D_2O, labile hydrogens in the protein are replaced with deuteriums at varying rates depending on hydrogen bonding and solvent accessibility. The interest in this technique has been significantly heightened by the introduction of mass spectrometry methods for analyzing deuterium incorporation and by the development of deuterium labeling followed by pepsin digestion which localizes exchange to short fragments of the protein (*39*, *40*). This technique allows amide hydrogen exchange studies of large proteins with high sensitivity. It is unique in that it is capable of easily detecting different conformational states (*41*).

Protein hydrogen exchange in the native state involves a two-step process in which a structural change allows isotope exchange (*37*). The structural change may be localized in a small region, facilitating the exchange of one or several amide hydrogens within this segment, or it may involve a global unfolding of a domain, making way for the exchange of all its amide hydrogens. The two mechanisms may operate in parallel in different regions of a protein. The two steps required for amide hydrogen exchange are illustrated in the following scheme (*42*)

$$\mathrm{F(H)} \underset{k_{cl}}{\overset{k_{op}}{\rightleftharpoons}} \mathrm{U(H)} \xrightarrow[k_c]{D_2O} \mathrm{U(D)} \underset{k_{op}}{\overset{k_{cl}}{\rightleftharpoons}} \mathrm{F(D)}$$

where F and U refer to the folded and unfolded forms, respectively. If $k_{cl} \gg k_c$, the structural change facilitating hydrogen exchange occurs many times before isotopic exchange takes place and the exchange is described by EX2 kinetics (*42*, *43*). This EX2 kinetics leads to a random distribution of deuterium among the peptides, and the isotope pattern observed in the mass spectra of peptides partially deuterated via such a mechanism will be binomial. In contrast, if $k_{cl} \ll k_c$, all sites exposed to the deuterated solvent will undergo isotopic exchange in the first opening. This form of isotope exchange is denoted as EX1 kinetics. The mass spectra of peptides undergoing isotope exchange by EX1 kinetics may have a bimodal distribution of isotopic peaks (*41*). The two envelopes of isotope peaks correspond to little and fully exchanged populations. H−D exchange followed by mass spectrometry measurements has been successfully used to analyze protein native conformational dynamics (*40*, *44*, *45*) and to detect conformational changes upon ligand binding (*46*, *47*) and transient protein folding intermediates of several proteins: hen lysozyme (*41*, *48*), cytochrome *c* (*49*), and apomyoglobin (*50*). These studies have demonstrated that the combination of H−D exchange and ESI-MS measurements of whole proteins can be a sensitive probe of protein global conformation, complementary to that obtained by circular dichroism (*51*) and NMR (*41*). Several groups have used this method in combination with several other techniques to detect and study molten globule conformations (*52*−*54*). The H−D exchange technique combined with proteolysis has been used to study conformational changes in the unfolding of aldolase (*55*, *56*).

Our study describes measurements of the equilibrium and kinetic GdmHCl-induced unfolding of MM-CK, monitored by intrinsic fluorescence, ANS binding, and far-UV CD. These data have been compared to those obtained under similar conditions with amide hydrogen exchange experiments. It was found that in 0.8 M GdmHCl, a concentration at which the molten globule state is maximally populated, the protein has a highly fluctuating structure, allowing a total deuteration under our experimental conditions.

MATERIALS AND METHODS

Protein Preparation. Creatine kinase from rabbit muscle (MM-CK) was purchased from Roche. The enzyme was desalted by using a PD10 Sephadex G25 column (Pharmacia) equilibrated in 50 mM Tris-HCl buffer (pH 7) or 20 mM Tris-AcOH, 0.1 mM EDTA buffer (pH 7.4). The protein concentration was estimated as described previously (*57*) or using a molar extinction coefficient of 76 000 M^{-1} cm^{-1} at 280 nm for MM-CK.

Materials. ATP and EDTA were purchased from Roche. D_2O (99.9%) and chloroacetic acid (99%) were purchased from Aldrich, and ANS, TFA, DTT, and creatine were from Sigma. GdmHCl and Tris were purchased from Interchim, and acetonitrile was from SDS.

Creatine Kinase Activity. MM-CK activity was determined using a pHstat method (*58*). Enzyme activity was measured at 30 °C and pH 8.8 using 4 mM MgATP and 40 mM creatine as substrates. Samples treated with GdmHCl were diluted at least 100-fold into the assay mixture for determination of MM-CK activity. We found that the residual concentration of GdmHCl, a competitive inhibitor of CK, does not affect the enzymatic activity significantly (*29*).

Equilibrium Unfolding by GdmHCl. Samples of 2 μM MM-CK were incubated with 50 mM Tris-HCl buffer (pH

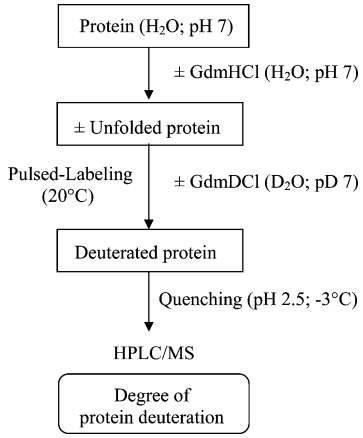

FIGURE 1: Experimental procedure used to determine the degree of deuteration of creatine kinase destabilized in GdmHCl by pulse-labeling hydrogen exchange coupled to mass spectrometry.

7) containing 0.1 mM EDTA, 5 mM DTT, and various concentrations of GdmHCl. To ensure that equilibrium has been attained, all experiments described below were performed after incubation at 20 °C for 19 h.

Kinetics of Unfolding by GdmHCl. Samples of 2 μM MM-CK were incubated at 20 °C for different times with 50 mM Tris-HCl buffer (pH 7) containing a final concentration of DTT of 2.5 mM and various concentrations of GdmHCl (conditions similar to those used for hydrogen−deuterium exchange experiments).

Intrinsic Fluorescence Measurements. Protein intrinsic fluorescence measurements were carried out on a Hitachi F-4500 spectrofluorimeter as previously described (*34*) with a final protein concentration of 2 μM at 20 °C. The excitation wavelength was 295 nm.

The "phase diagram" method of Burstein, which is very sensitive in detecting intermediate states, was used to analyze fluorescence data (*36*). This diagram plots the fluorescence intensity (*I*) at a wavelength chosen from one side of the fluorescence emission peak versus the intensity at another wavelength located on the other side of the peak. Its nonlinearity reflects sequential transformations between intermediate states during the denaturation process. In our case, the intensity at 365 nm (I_{365}) was plotted versus the intensity at 320 nm (I_{320}) using an excitation wavelength of 295 nm.

ANS Binding Measurements. ANS (final concentration of 310 μM) in methanol was added to the protein samples (final protein concentration of 2 μM), and the ANS fluorescence was recorded at 495 nm with an excitation wavelength of 395 nm. All spectra were corrected for the free ANS fluorescence. For unfolding kinetics, ANS was added to CK after a determined denaturation time.

CD Spectroscopy. CD measurements were recorded on a Jobin Yvon CD6 spectropolarimeter. The ellipticity was measured at 222 nm. MM-CK (final concentration of 3 μM) was incubated at 20 °C for different times with 50 mM Tris-HCl buffer (pH 7) containing a final DTT concentration of 2.5 mM and 0.8 M GdmHCl.

Deuterium Exchange. The procedure used to pulse-label MM-CK with deuterium following denaturation by GdmHCl for various times is illustrated in Figure 1. MM-CK (80 μM) in 50 mM Tris-HCl/H_2O buffer (pH 7) was diluted (1/1, v/v) into 50 mM Tris-HCl/H_2O buffer (pH 7 and 20 °C) containing 5 mM DTT and the amount of GdmHCl required to obtain final concentrations of 0, 0.4, 0.6, 0.8, 1, or 3 M. Following this unfolding period, the solution was diluted 1/20 with D_2O labeling solution [50 mM Tris-DCl/D_2O and 0, 0.4, 0.6, 0.8, 1, or 3 M GdmDCl (pD 7) at 20 °C] to label the protein. All pD measurements are given as the values read from the pH meter with no adjustment for isotope effects (*59*). The deuterated labeling solution containing GdmHCl was prepared by concentration to $^1/_5$ of its initial volume using a vacuum concentrator (SpeedVac). The concentrated solution was reconstituted with D_2O and concentrated again. This step was repeated three times. Experimental considerations for designing pulse labeling experiments in which deuterium levels at peptide amide linkage are determined by mass spectrometry have been discussed by Deng *et al.* (*60*). Isotope exchange was quenched after various times ranging from 10 s to 60 min by the addition of cold 0.2 M chloroacetic acid (H_2O, pH 2) to decrease the pH to 2.5 and by decreasing the temperature to −3 °C in an ice/H_2O/ammonium sulfate bath. The MM-CK final concentration was 1.86 μM. The sample (280 pmol) was analyzed immediately by HPLC−electrospray ionization mass spectrometry. The HPLC column was a reversed phase concentration microcolumn (C4, 3 mm × 8 mm, Michrom Bioresources). The HPLC column and the entire injector assembly were packed in ice to minimize H−D exchange at peptide amide linkages during analysis. Note that rate constants for exchange at peptide amide linkages increase 3-fold for each 10 °C increase (*61*). A 2 min desalting step (100% mobile phase A containing 0.1% TFA/H_2O) at a rate of 500 μL/min was used before the HPLC system was connected to the mass spectrometer. MM-CK was then eluted at a rate of 200 μL/min directly into the mass spectrometer within 8 min with 60% phase B containing 90% acetonitrile, 0.1% TFA, and H_2O.

Back-Exchange Controls. With each set of samples, an undeuterated (0% reference) control and a totally deuterated (100% reference) control were also analyzed (*39*). The 100% reference in which all exchangeable hydrogens have been replaced with deuterium was prepared by incubating the protein in 50 mM Tris-DCl/D_2O buffer (pD 2.5) at 35 °C for 3 h. The 0% reference was prepared by mixing a stock solution of MM-CK with buffer containing no deuterium. These controls were also quenched at the same final percentage of deuterium as the samples to correct for gain and loss of deuterium.

Correction was done according to eq 1

$$D = \frac{m - m_{0\%}}{m_{100\%} - m_{0\%}} N \qquad (1)$$

where D is the deuterium content of the protein, m, $m_{0\%}$, and $m_{100\%}$ are the average molecular masses of the same protein in the sample, the undeuterated form, and the totally deuterated form, respectively, and N is the number of exchangeable peptide amide hydrogens in the protein (number of peptide bonds not involving Pro residues). The HPLC step was performed with protiated solvants, thereby removing deuterium from side chains and amino and carboxy termini that exchange much faster than amide linkages (*61*). Therefore, the increase in mass is a direct measurement of the level of deuteration at peptide amide linkages.

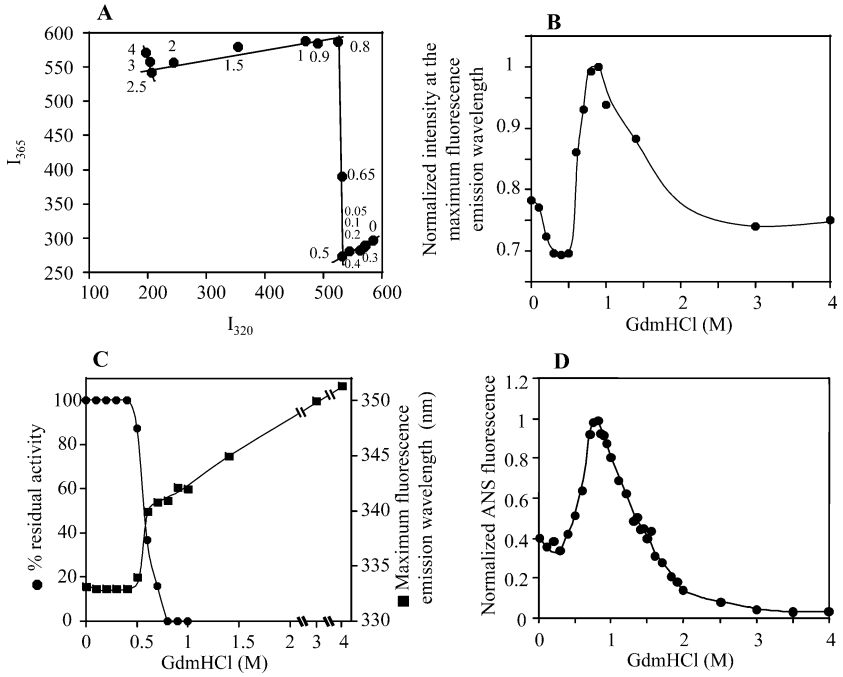

FIGURE 2: Effect of GdmHCl on equilibrium unfolding of creatine kinase. (A) Phase diagram representing the equilibrium unfolding of creatine kinase induced by an increase in GdmHCl concentration. I_{320} and I_{365} correspond to the intensities for each concentration of GdmHCl at 320 and 365 nm, respectively. Denaturant concentrations (molar) are indicated next to the corresponding symbol. Each segment represents an all-or-none transition between two different conformations. (B) Variation of the intensity at the maximum fluorescence emission wavelength during the equilibrium unfolding of MM-CK by GdmHCl. The excitation wavelength was 295 nm. (C) The residual activity of MM-CK (●) was measured with the pHstat method, and the maximum fluorescence emission wavelength (■) was determined using an excitation wavelength of 295 nm to selectively excite tryptophan residues. (D) Measurements of ANS binding to creatine kinase unfolded at equilibrium. Aliquots of a 25 mM methanolic ANS solution were added to the spectrofluorimeter cuvette (final ANS concentration of 310 μM). Samples were excited at 395 nm, and the ANS fluorescence intensities were recorded at 495 nm. For all experiments, MM-CK (final enzyme concentration of 2 μM) was unfolded by incubation for 19 h at 20 °C at various concentrations of GdmHCl in 50 mM Tris-HCl, 0.1 mM EDTA, and 5 mM DTT (pH 7.0).

Data Analysis. Deuterium levels were plotted versus the exchange time and fitted to a three-exponential expression according to eq 2:

$$D = N - \sum a_i \exp(-k_i t) \quad (2)$$

where a_i is the number of deuteriums that can be exchanged with a similar rate constant, k_i, and N is the sum of the a_i values (corresponding to the number of peptide amide linkages for which the hydrogen exchange rate is measurable). The a_i values were rounded up to the nearest integer.

Mass Spectrometry. Analyses of MM-CK were performed using an API III+ triple-quadrupole mass spectrometer (Perkin-Elmer Sciex) equipped with a nebulizer-assisted electrospray ionization interface. The instrument was calibrated using polypropylene glycol. The ion spray voltage was set at 5 kV, and the orifice voltage was 80 V for MM-CK analysis. Mass spectra were recorded from *m*/*z* 900 to 1250 using a step of *m*/*z* 0.5 and a dwell time of 2 ms/step. The nebulizer gas was nitrogen to prevent back-exchange during the ionization−desorption process. Mass spectra were acquired using a Macintosh Quadra 950 data system, and molecular masses were calculated using Mac Spec software (Perkin-Elmer Sciex).

RESULTS

Equilibrium Unfolding. The complexity of the GdmHCl-induced unfolding process is illustrated in Figure 2A by a phase diagram showing the dependence of the tryptophan fluorescence emission at 365 nm versus that at 320 nm (*36*). This phase diagram shows significant changes in the characteristics of the intrinsic fluorescence. Between 0 and 0.5 M GdmHCl, the intensity at 320 nm exhibits a small decrease. However, between 0.5 and 0.8 M GdmHCl, I_{365} increases greatly. Between 0.8 and 2.5 M, there is a large decrease in I_{320}. Above 2.5 M GdmHCl, I_{365} increases again. Each linear portion of the diagram describes a two-state transition. For our experimental conditions, four linear parts can be drawn (from 0 to 0.5, from 0.5 to 0.8, from 0.8 to 2.5, and from 2.5 to 4). The transitions do not occur at the same GdmHCl concentrations as those observed by Kuznetsova *et al*. (*36*), probably because of differences in pH and temperature. Figure 2B shows the variation of the intensity at the maximum emission wavelength in increasing concentrations of GdmHCl. Between 0 and 0.5 M GdmHCl, a slight decrease in the intensity is observed. The increased intensity observed around 0.8 M GdmHCl, where the CK dimer is dissociated, is related to perturbations of the microenvironment of tryptophan residues. Above 2.5 M GdmHCl, the intensity level is low and constant. These results indicate the presence of five states of MM-CK during the denaturation: the native protein between 0 and 0.5 M GdmHCl, the completely unfolded protein above 2.5 M GdmHCl, and three intermediate states reaching maximum populations at 0.5, 0.8, and 2.5 M GdmHCl. At the protein concentration that was used (2 μM), no aggregate formation was observed. Perturbations to the CK three-dimensional structure can also be sensitively monitored using enzymatic

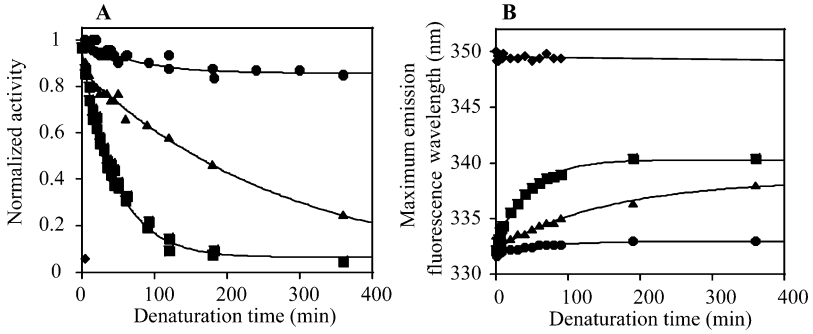

FIGURE 3: Effect of GdmHCl on the unfolding kinetics of creatine kinase. (A) The residual activity of MM-CK, normalized to the native protein value, was measured at different concentrations of GdmHCl. The data were fitted to the equation $A_t = a \exp(-kt) + b$. (B) The maximum fluorescence emission wavelength, at different concentrations of GdmHCl, was determined using an excitation wavelength of 295 nm. For all experiments, MM-CK was unfolded by incubation at various concentrations of GdmHCl: 0.5 (●), 0.65 (▲), 0.8 (■), and 3 M (◆) in 50 mM Tris-HCl and 2.5 mM DTT (pH 7.0). The final enzyme concentration was 2 μM. The data were fitted to the equation $F_t = (F_F - F_U) \exp(-kt) + F_U$, where F_F and F_U are the λ_{max} values of folded and unfolded MM-CK, respectively.

activity and λ_{max} measurements (*29*). Since the denaturing effect of low to moderate GdmHCl concentrations is very much dependent on temperature, those measurements have been carried out at a controlled temperature (20 °C). CK begins to lose its activity above 0.4 M GdmHCl and is fully inactivated at 0.8 M denaturant (Figure 2C). When the enzyme is incubated in <0.5 M GdmHCl, its maximum fluorescence emission wavelength (λ_{max}) is 332 nm, indicating that the four tryptophan residues remain mostly buried inside the protein (Figure 2C). Although the enzyme is completely inactivated in 0.8 M GdmHCl, it is not fully denatured, as indicated by its λ_{max} of 341 nm. For higher denaturant concentrations, the λ_{max} increases up to 350 and 352 nm at 3 and 4 M GdmHCl, respectively. The binding of the fluorescent hydrophobic probe ANS was assessed at various GdmHCl concentrations (Figure 2D). This extrinsic probe is often used to show evidence of molten globule, a structural intermediate state with exposed hydrophobic regions to which ANS can bind thereby increasing its fluorescence quantum yield (*62*). The intensity of ANS fluorescence emission, which is low for the native enzyme, strongly increases up to 0.8 M GdmHCl and then decreases to a very low level where the fully denatured protein no longer binds the probe.

The comparison of the different equilibrium data (Figure 2) indicates that around 0.5 M GdmHCl the protein begins to lose its enzymatic activity, its λ_{max} begins to increase, and ANS is weakly bound. At 0.8 M denaturing agent, the enzyme is fully inactivated, its λ_{max} is 341 nm, and ANS binding is strong. These data indicate the presence of a molten globule state. The inactive intermediate present at 2.5 M GdmHCl has a λ_{max} around 350 nm, and it weakly binds ANS. The variations of the phase diagram (Figure 2A) and of the intensity measured at the emission λ_{max} (Figure 2B) both show that further structural modifications occur well above the GdmHCl concentration necessary for a total inactivation of the enzyme.

Unfolding Kinetics. The kinetics of enzyme inactivation and variation of fluorescence parameters were studied under similar conditions (Figure 3). Figure 3A shows that the degree of inactivation depends on GdmHCl concentration; it is low in 0.5 M GdmHCl and nearly complete in 0.8 and 3 M GdmHCl. The equilibrium between active and inactive states of CK is in favor of the active form in 0.5 M GdmHCl, but shifts to the inactive form above 0.65 M GdmHCl.

Table 1: Rate Constants of MM-CK Denaturation Kinetics in 0.8 M GdmHCl for Different Parameters[a]

	rate constant (min^{-1})
inactivation	0.021 ± 0.001
disappearance of the low-mass species	0.023 ± 0.002
appearance of the high-mass species	0.026 ± 0.003
λ_{max} variation	0.022 ± 0.001
ANS binding	0.031 ± 0.001
variation of ellipticity at 222 nm	0.027 ± 0.001

[a] All data were fitted to a monoexponential expression.

λ_{max} variations are analyzed in Figure 3B. The equilibrium value in 3 M GdmHCl (350 nm) is attained in less than 20 s, whereas in 0.5 M GdmHCl, the λ_{max} increased within 1 h by only 1 nm from its native value, 332 nm, in parallel with a loss of activity of ~15%. The rate and extent of denaturation increase as the GdmHCl concentration is increased from 0.5 to 0.65 M and then to 0.8 M. At this latter concentration, the kinetics of enzyme inactivation and λ_{max} variation were not dependent on the protein concentration (data not shown), indicating that the unfolding process does not involve an equilibrium with a rate-limiting monomer−dimer transition.

The kinetics of the decrease in ellipticity at 222 nm and of the increase in the ANS fluorescence at 495 nm due to probe binding have been studied in a similar way in 0.8 M GdmHCl (not shown). The data have been fitted to first-order kinetics. The rate constants of variation of these parameters, represented in Table 1, are very similar to those of inactivation and variation of λ_{max}.

In summary, when CK is denatured in 0.8 M GdmHCl, it strongly binds ANS, it has a λ_{max} of 341 nm, higher than that of the native state (332 nm), but lower than that of the fully denatured protein (352 nm), and its ellipticity at 222 nm is 55% of that of the native protein. All of these data confirm that a molten globule state of CK is present under these conditions.

Hydrogen−Deuterium Exchange. To further characterize the pattern of CK denaturation at low GdmHCl concentrations and the structure of the molten globule intermediate observed at 0.8 M GdmHCl, hydrogen−deuterium exchange experiments were carried out with analysis by mass spectrometry.

Deconvoluted mass spectra of CK incubated under native or denaturing conditions are presented in Figure 4. The

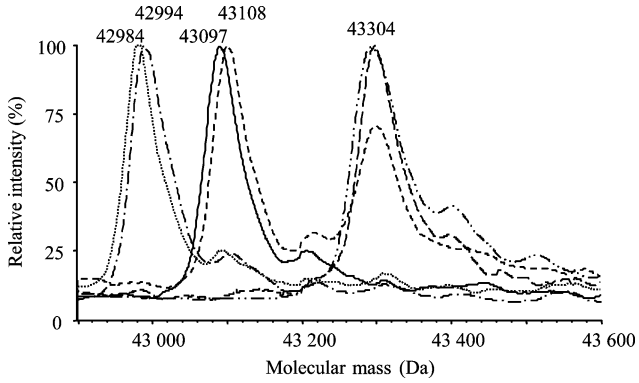

FIGURE 4: Reconstructed spectra of MM-CK obtained by the deconvolution of the electrospray ionization mass spectra. MM-CK was pulse-labeled in D_2O for 120 s following incubation in 0 M GdmHCl (—), 0.8 M GdmHCl for 30 min (- - -), and 3 M GdmHCl for 10 min (— — —). Reconstructed spectra of non-deuterated MM-CK (···), the 0% reference (0% ref) (—·—), and completely deuterated MM-CK (100% ref) (—··—) are also presented. The minor peak observed after the main ones is probably due to an adduct.

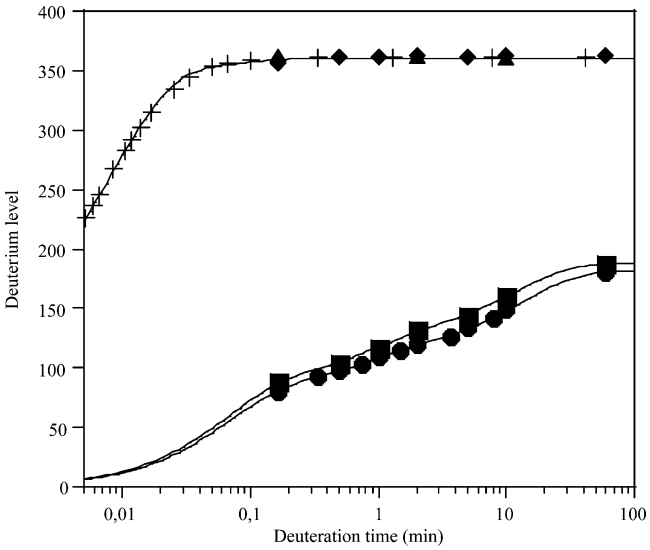

FIGURE 5: Deuterium levels in MM-CK following incubation of the protein in D_2O for 10 s to 60 min. The deuterium level is corrected for deuterium gain and/or loss during analysis. MM-CK was incubated in 0 M GdmHCl (●), 0.8 M GdmHCl for 30 min (■ and ◆), and 3 M GdmHCl for 10 min (▲). The theoretical deuterium level expected for the unfolded protein (+) was calculated by using the HXPEP program. The lines correspond to the best fit to eq 2.

average molecular mass measured for CK with a natural abundance of isotopes was 42 984 ± 4 Da (calculated M_r of 42 982 Da). The average molecular mass of the 0% reference (i.e., nondeuterated CK that has been treated under conditions similar to those of the incubated samples) was 42 994 Da. There is a small increase in the level of deuteration during the quenching period (10 Da). After a 120 s incubation in D_2O, the mass of the native enzyme increased to 43 097 Da. Since deuteriums located in the side chains, as well as those at the N- and C-termini of the protein, were replaced with protons during the HPLC step, the increase in the molecular mass of CK (103 Da) reflects only the deuteration of peptide amide linkages. The 100% reference (43 304 Da) has incorporated 320 deuteriums, which is significantly fewer than the 361 exchangeable amide hydrogens in MM-CK. The difference (41 deuterons) is due to back-exchange with solvent protons during the analytical phase. When CK was partially unfolded in 0.8 M GdmHCl for 30 min followed by H−D exchange for 120 s, two mass envelopes were observed: a low-mass envelope at 43 108 Da and a high-mass envelope at 43 304 Da. The low-mass species observed at 0.8 M GdmHCl has a slightly but reproducibly higher mass than the native deuterated protein (between 5 and 11 Da for an expected mass measurement error of ∼4 Da). An unfolded sample of CK denatured for 10 min in 3 M GdmHCl exhibited only one peak at 43 304 Da. Thus, the high-mass species observed in 0.8 M GdmHCl, the species unfolded in 3 M GdmHCl, and the totally deuterated sample (100% reference) have the same mass.

Figure 5 shows the kinetics of deuteration of native CK and of CK incubated in 0.8 and 3 M GdmHCl for 30 and 10 min, respectively. The minimal deuteration time required to obtain reproducible results was 10 s. The raw data were corrected for deuterium gain or loss during the quenching and desalting phases (eq 1), and the curves were fitted to eq 2. For the native enzyme, 181 of the 361 total amide hydrogens were replaced with deuterium within 1 h. At least three steps with well-resolved rate constants can be detected in the kinetics: 79 amide hydrogens are exchanged with a rate constant of 15.6 min^{-1}, 31 replaced with deuterium at a rate constant of 1.4 min^{-1}, and 71 replaced with a very low rate constant of 0.06 min^{-1}. The 180 remaining amide hydrogens are not exchanged or exchanged with such low rate constants that they could not be determined under the experimental conditions presented here. The shape of the deuteration kinetics observed for the low-mass species in 0.8 M GdmHCl is similar to that of the native one. However, the total amount of deuteriums incorporated was increased by 7 to 188 after deuteration for 1 h. This increase in the level of deuteration resulted from an increase of approximately five and eight deuteriums exchanged in the two faster phases and a decrease of approximately six slowly exchangeable amide hydrogens. For the high-mass species observed in 0.8 M GdmHCl, as well as for 3 M denatured CK, deuteration of peptide bonds is nearly total at the first measurement time. For comparison, the theoretical deuteration kinetics of the nonstructured polypeptide calculated using Bai *et al*. (*61*) data with the HXPEP program written by Z. Zhang is drawn in Figure 5.

To look for the existence of deuterated species other than those described by the results in Figure 4, CK denatured in various GdmHCl concentrations for 10 min was incubated in D_2O buffer for 10 s. Figure 6 clearly shows that, whatever the denaturant concentration, no species other than those already described was detected. Only two peaks are present in variable proportions. The low-mass species corresponds to the only peak detected in 0.4 and 0.6 M GdmHCl under these experimental conditions. Although it is the major peak at 0.8 M, it disappeared at 1.5 M GdmHCl (not shown). The high-mass species having the same mass as the fully deuterated protein appears in 0.8 M GdmHCl, is dominant in 1 M GdmHCl, and is the single species observed in 3 M GdmHCl. Thus, the rate of conversion of the low-mass species into the high-mass species is dependent on the GdmHCl concentration.

The kinetics of MM-CK denaturation in 0.8 M GdmHCl was studied in more detail by pulse labeling for 10 s (Figure

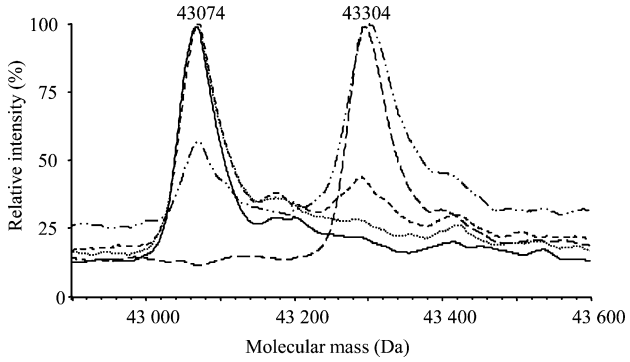

FIGURE 6: Reconstructed spectra of MM-CK obtained by the deconvolution of the electrospray ionization mass spectra. MM-CK was pulse-labeled in D_2O for 10 s following denaturation for 10 min at different concentrations of GdmHCl: 0.4 (—), 0.6 (•••), 0.8 (- - -), 1 (—••—), and 3 M (— — —).

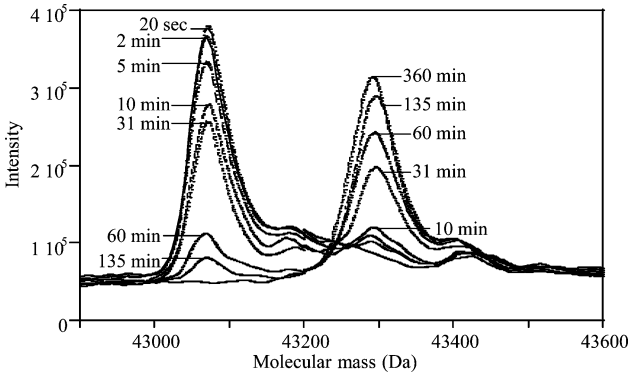

FIGURE 7: Unfolding kinetics of MM-CK in 0.8 M GdmHCl for 20 s to 360 min. The reconstructed spectra of MM-CK were obtained by the deconvolution of the electrospray ionization mass spectra. The protein was pulse-labeled in D_2O for 10 s. Denaturation times are given on each mass spectrum.

7). Again, only two peaks were observed. The low-mass species, which corresponds to the only peak observed after a denaturation time of 20 s, disappeared with a correlated increase in the level of the high-mass species, which corresponds to the only peak remaining after 360 min. No evidence for a species with an intermediate level of deuteration can be found.

DISCUSSION

Behavior of Native or Denatured MM-CK in D_2O. When solubilized in a deuterated buffer, native MM-CK exchanges 69 of its amide protons in 10 s and 103 in 120 s, corresponding to 22 and 32% of its 320 exchanged amide protons, respectively. Thus, a significant number of MM-CK protons could be exchanged under native conditions. This is surprising with regard to its high resistance to proteases, but suggests a relatively high dynamics in at least some regions of the protein.

When MM-CK was denatured in 0.4−3 M GdmHCl for 10 min, only two deuterated species can be observed in changing proportions. Only these two species were found when the H−D exchange was carried out after different denaturation periods in 0.8 M GdmHCl. Thus, the proportions of the two MM-CK populations are strongly dependent on GdmHCl concentration and denaturation time.

Whatever the different incubation conditions, the masses of these two species were constant, although their relative intensities changed. This bimodal pattern, observed between 0.8 and 1.5 M GdmHCl, is typical of an H−D exchange process occurring with an EX1 mechanism. That is, the structure interchange time is longer than the labeling time, which is longer than the time required for hydrogen exchange in an unprotected polypeptide. Finding a low-mass peak corresponding to the less deuterated protein (i.e., protected form) and a high-mass peak corresponding to the totally deuterated protein (i.e., unprotected form) is consistent with these conditions. Indeed, EX1 kinetics are most frequently observed when proteins are destabilized by addition of a denaturing agent, an acidic or basic pH, or a high temperature (*41*, *63*, *64*). Equilibrium as well as kinetic GdmHCl-induced unfolding of rabbit muscle CK was studied. The unfolding process involves several partially folded intermediates, one of them resembling the molten globule state. Thus, despite the evidence found for the presence of different intermediates on the unfolding pathway of MM-CK, H−D exchange experiments analyzed by mass spectrometry clearly indicated that no more than two deuterated species are present during GdmHCl denaturation. Obviously, ESI-MS is a very good technique for obtaining the distribution of masses within a population of protein molecules that had undergone hydrogen exchange, and thus, it is a good method for obtaining evidence for intermediate states that have different H−D exchange properties (*41*). It has been shown that mass spectra of aldolase destabilized in 3.5 M urea exhibited four peaks and that the intensities changed with denaturation time. Each peak corresponded to a particular unfolded form of the protein (*64*). The first peak corresponds to the native undeuterated aldolase (0% reference) and the fourth to the nearly completely deuterated protein, and the two other peaks represent two partially unfolded states of aldolase. The pattern that we found with MM-CK is quite different since we found a maximum of two peaks whatever the denaturation and deuteration times and the denaturant concentration. We have thus to reconcile the existence of several intermediates with that of only two deuterated species. One likely explanation is that other conformational states are so dynamic that all sites are labeled within 10 s. Other conformational states may become observable with shorter pulse times (<2 s), which would require the use of a quench-flow system.

Characterization of the Molten Globule State of MM-CK. The link among inactivation, λ_{max} variation, and the relative proportion of the low-mass and high-mass peaks as a function of denaturation time was more thoroughly investigated at 0.8 M GdmHCl, where the molten globule state is maximally populated. The areas under the two peaks presented in Figure 7 were estimated and plotted as a function of time in Figure 8 together with the variation of activity and λ_{max}. For an easier comparison, all the parameters presented in this figure have been normalized to their maximum variation in 0.8 M GdmHCl. The low-mass species slowly disappears and is converted into the high-mass species. An equivalent proportion of the two species is found after a 30 min incubation period. The decrease of the less exchanged form clearly parallels the loss of activity, and both parameters approach their minimal values after 3 h. This pattern suggests that the less exchanged species, which has gained no more than 10 deuteriums as compared to the deuterated native protein, is the only active form. Thus, the conformational change, which allows this additional deuteration, is not sufficient to

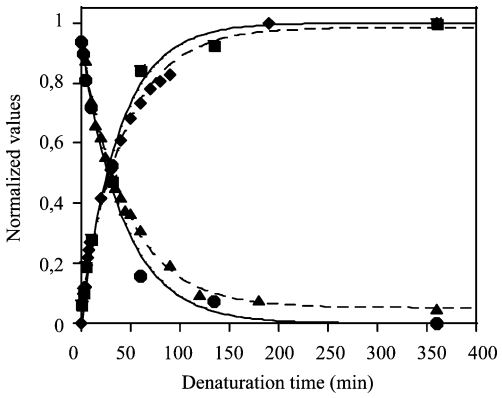

FIGURE 8: Comparison of the unfolding kinetics data for MM-CK incubated in 0.8 M GdmHCl: enzyme inactivation (▲), maximum fluorescence emission wavelength (◆), and proportions determined by deuterium exchange of two species present at this concentration of GdmHCl. The fractions of the low-mass species (●) and the high-mass species (■) were fitted to a monoexponential expression.

inactivate the enzyme or is easily reversible. For the other population of molecules, a major conformational perturbation, including the catalytic site, occurs and leads to total deuteration and inactivation. The appearance of the high-mass species is tightly correlated with the increase in the λ_{max} of the intrinsic fluorescence from 332 to 341 nm, with a partial decrease in the ellipticity at 222 nm and with the increased level of binding of ANS to CK. The rate constants of variation of all parameters summarized in Table 1 are very similar. This correlation is in agreement with the occurrence of simultaneous secondary and tertiary structural changes during unfolding of CK (*33*). Thus, after a 3 h denaturation period in 0.8 M GdmHCl, most of the CK molecules exist as a molten globule, which could be fully deuterated in a deuteration time of 10 s.

Far-UV circular dichroism analysis of the early folding intermediates of other proteins has shown the presence of important amounts of secondary structure, while H−D exchange indicated the presence of no or little hydrogen amide protection. The C-terminal proteolytic domain (F2) of the *Escherichia coli* tryptophan synthase β chain appears to exist as a molten globule that exhibits very low amide proton protection and yet contains a native secondary structure stabilized by hydrogen bonds (*65*). Removing the heme group of holomyoglobin destabilizes both its tertiary and secondary structure. Despite an α-helix content of ∼73% of that of holomyoglobin, only 4% of the labile hydrogens of apomyoglobin remain unexchanged after 30 min at pH 6 (*51*). In some cases (canine vs equine milk lysozyme), an enhanced protection and stability are caused by the strengthened cooperative interactions between helices (*66*). However, as discussed by Guijarro *et al*. (*65*), the observation of a completely deuterated molten globule state raises an apparent paradox. If the backbone conformation giving rise to the far-UV CD spectra of the molten globule is due to authentic secondary structures stabilized by hydrogen bonds, one would expect a large number of the backbone amide protons to be protected from deuterium exchange. Conversely, we observe no protection in our pulsed amide proton exchange experiments. This can be explained by the low stability of the existing secondary structures in the presence of GdmHCl. During the pulsed exchange, a rapid equilibrium exists between open and closed states, and protein molecules spend a significant portion of time in a partly folded or unfolded state where H−D exchange can occur. In contrast to CD, which measures the average amount of α-helical content, H−D exchange analyzed by ESI-MS is cumulative. The number of exchanged amide protons reflects the presence of fluctuating structures (*51*). Thus, the secondary structure of the CK molten globule must have high dynamics so that all its amide hydrogens can be fully exchanged. Using site-directed mutagenesis, we have previously shown that the CK dimeric state ensures the maximal stability of the subunits (*67*). This may induce an enhanced protection against H−D exchange. Such a role of quaternary structure in the stabilization of dimeric proteins has been observed for ascorbate oxidase and procaspase (*68*, *69*). The assembly of monomers into a dimeric molecule would then play a fundamental role by driving the final organization of the tertiary structure.

On the basis of our results, we can propose a scheme describing the very first events occurring during guanidinium chloride-induced partial denaturation. When incubated in 0.8 M GdmHCl, the active dimer is slightly modified. This modification, which is evidenced by the low increase in amide exchangeability, either has no effect on enzyme activity or is rapidly reversed in the assay medium. It has no immediate consequence on the quaternary structure. It would, however, increase the sensitivity of CK to GdmHCl which would then bind to an otherwise hidden region of the protein structure, leading to monomerization (when denatured at equilibrium in 0.8 M GdmHCl, CK is in a monomeric state). Once monomerized, the enzyme has no activity and is unable to renature during the assay due to the low monomer concentration, which precludes the formation of an appreciable amount of active dimer. The fact that the activity and the less exchangeable form are lost at the same rate further strengthens our previous conclusion about the stabilizing role of the quaternary structure.

Work to localize the small but reproducible increase in the level of deuteration is currently in progress, via the use of H−D exchange and proteolysis. The concerned regions could be located in areas with little structure such as the N- or C-terminal end or the surface loops of MM-CK.

REFERENCES

1. Price, N. C. (1994) Assembly of multi-subunit structures, in *Mechanisms of Protein Folding* (Pain, R. H., Ed.) IRL Press, Oxford, U.K.
2. Ptitsyn, O. B. (1987) Protein folding: hypotheses and experiments, *J. Protein Chem. 6*, 273−293.
3. Kuwajima, K. (1989) The molten globule state as a clue for understanding the folding and cooperativity of globular-protein structure, *Proteins 6*, 87−103.
4. Kim, P. S., and Baldwin, R. L. (1990) Intermediates in the folding reactions of small proteins, *Annu. Rev. Biochem. 59*, 631−660.
5. Ptitsyn, O. B., Pain, R. H., Semisotnov, G. V., Zerovnik, E., and Razgulyaev, O. I. (1990) Evidence for a molten globule state as a general intermediate in protein folding, *FEBS Lett. 262*, 20−24.
6. Ptitsyn, O. B. (1995) Molten globule and protein folding, *Adv. Protein Chem. 47*, 83−229.
7. Martin, J., Langer, T., Boteva, R., Schramel, A., Horwich, A. L., and Hart, F. U. (1991) Chaperonin-mediated protein folding at the surface of GroEL through a molten globule-like intermediate, *Nature 352*, 36−42.
8. Evans, P. A., and Radford, S. E. (1994) Probing the structure of folding intermediates, *Curr. Opin. Struct. Biol. 4*, 100−106.

9. Kay, M. S., and Baldwin, R. L. (1996) Packing interactions in the apomyoglobin folding intermediate, *Nat. Struct. Biol. 3*, 439−445.
10. Wyss, M., Smeitink, J., Wevers, R. A., and Wallimann, T. (1992) Mitochondrial creatine kinase: A key enzyme of aerobic energy metabolism, *Biochim. Biophys. Acta 1102*, 119−166.
11. Fritz-Wolf, K., Schnyder, T., Wallimann, T., and Kabsch, W. (1996) Structure of mitochondrial creatine kinase, *Nature 381*, 341−345.
12. Eder, M., Fritz-Wolf, K., Kabsch, W., Wallimann, T., and Schlattner, U. (2000) Crystal structure of human ubiquitous mitochondrial creatine kinase, *Proteins 39*, 216−225.
13. Rao, J. K. M., Bujacz, G., and Wlodawer, A. (1998) Crystal structure of rabbit muscle creatine kinase, *FEBS Lett. 439*, 133−137.
14. Eder, M., Schlattner, U., Becker, A., Wallimann, T., Kabsch, W., and Fritz-Wolf, K. (1999) Crystal structure of brain-type creatine kinase at 1.41 Å resolution, *Protein Sci. 8*, 2258−2269.
15. Tisi, D. D., Bax, B. B., and Loew, A. A. (2001) The three-dimensional structure of cytosolic bovine retinal creatine kinase, *Acta Crystallogr. D57*, 187−193.
16. Shen, Y. Q., Tang, L., Zhou, H. M., and Lin, Z. J. (2001) Structure of human muscle creatine kinase, *Acta Crystallogr. D57*, 1196−1200.
17. Webb, T. I., and Morris, G. E. (2001) Structure of an intermediate in the unfolding of creatine kinase, *Proteins 42*, 269−278.
18. Lahiri, S. D., Wang, P. F., Babbitt, P. C., McLeish, M. J., Kenyon, G. L., and Allen, K. N. (2002) The 2.1 Å structure of *Torpedo californica* creatine kinase complexed with the ADP−Mg^{2+}−NO_3^- creatine transition-state analogue complex, *Biochemistry 41*, 13861−13867.
19. Kabsch, W., and Fritz-Wolf, K. (1997) Mitochondrial creatine kinase: A square protein, *Curr. Opin. Struct. Biol. 7*, 811−818.
20. Yousef, M. S., Clark, S. A., Pruett, P. K., Somasundaram, T., Ellington, W. R., and Chapman, M. S. (2003) Induced fit in guanidino kinases: comparison of substrate-free and transition state analog structures of arginine kinase, *Protein Sci. 12*, 103−111.
21. Leydier, C., Andersen, J. S., Couthon, F., Forest, E., Marcillat, O., Denoroy, L., Vial, C., and Clottes, E. (1997) Proteinase K processing of rabbit muscle creatine kinase, *J. Protein Chem. 16*, 67−74.
22. Lebherz, H. G., Burke, T., Shackelford, J. E., Strickler, J. E., and Wilson, K. J. (1986) Specific proteolytic modification of creatine kinase isoenzymes. Implication of C-terminal involvement in enzymic activity but not in subunit-subunit recognition, *Biochem. J. 233*, 51−56.
23. Wyss, M., James, P., Schlegel, J., and Wallimann, T. (1993) Limited proteolysis of creatine kinase: Implications for 3-dimensional structure and for conformational substates, *Biochemistry 32*, 10727−10735.
24. Williamson, J., Greene, J., Cherif, S., and Milner-White, E. J. (1977) Heterogeneity of rabbit muscle creatine kinase and limited proteolysis by proteinase K, *Biochem. J. 167*, 731−737.
25. Price, N. C., and Stevens, E. (1982) The refolding of denatured rabbit muscle creatine kinase search for intermediates in the refolding process and effect of modification at the reactive thiol group on refolding, *Biochem. J. 201*, 171−177.
26. Webb, T., Jackson, P. J., and Morris, G. E. (1997) Protease digestion studies of an equilibrium intermediate in the unfolding of creatine kinase, *Biochem. J. 321*, 83−88.
27. Morris, G. E., and Cartwright, A. J. (1990) Monoclonal antibody studies suggest a catalytic site at the interface between domains in creatine kinase, *Biochim. Biophys. Acta 1039*, 318−322.
28. Fontana, A., Polverino de Loreto, P., De Filippis, V., Scarmella, E., and Zambonin, M. (1997) Probing partly folded states of proteins by limited proteolysis, *Folding Des. 2*, 17−26.
29. Couthon, F., Clottes, E., Ebel, C., and Vial, C. (1995) Reversible dissociation and unfolding of dimeric creatine kinase isoenzyme MM in guanidine hydrochloride and urea, *Eur. J. Biochem. 234*, 160−170.
30. Gross, M., Lustig, A., Wallimann, T., and Furter, R. (1995) Multiple-state equilibrium unfolding of guanidino kinases, *Biochemistry 34*, 10350−10357.
31. Clottes, E., Leydier, C., Couthon, F., Marcillat, O., and Vial, C. (1997) Denaturation by guanidinium chloride of dimeric MM-creatine kinase and its proteinase K-nicked form: evidence for a multiple-step process, *Biochim. Biophys. Acta 1338*, 37−46.
32. Zhou, J. M., Fan, Y. X., Kihara, K., Kimura, K., and Amemiya, Y. (1997) Unfolding of dimeric creatine kinase in urea and guanidine hydrochloride as measured using small-angle X-ray scattering with synchrotron radiation, *FEBS Lett. 415*, 183−185.
33. Fan, Y. X., Zhou, J. M., Kihara, H., and Tsou, C. L. (1998) Unfolding and refolding of dimeric creatine kinase: equilibrium and kinetic studies, *Protein Sci. 7*, 2631−2641.
34. Leydier, C., Clottes, E., Couthon, F., Marcillat, O., Ebel, C., and Vial, C. (1998) Evidence for kinetic intermediate states during the refolding of GdnHCl-denatured MM-creatine kinase. Characterization of a trapped monomeric species, *Biochemistry 37*, 17579−17589.
35. Zhang, Y. L., Fan, Y. X., Huang, G. C., Zhou, J. X., and Zhou, J. M. (1998) Equilibrium intermediates in the unfolding pathway of creatine kinase, *Biochem. Biophys. Res. Commun. 246*, 609−612.
36. Kuznetsova, I. M., Stepanenko, O. V., Turoverov, K. K., Zhu, L., Zhou, J. M., Fink, A. L., and Uversky, V. N. (2002) Unraveling multistate unfolding of rabbit muscle creatine kinase, *Biochim. Biophys. Acta 1596*, 138−155.
37. Englander, S. W., and Kallenbach, N. R. (1984) Hydrogen exchange and structural dynamics of proteins and nucleic acids, *Q. Rev. Biophys. 16*, 521−655.
38. Engen, J. R., and Smith, D. L. (2000) Investigating the higher order structure of proteins, *Methods in Mol. Biol. 146*, 95−112.
39. Zhang, Z., and Smith, D. L. (1993) Determination of amide hydrogen exchange by mass spectrometry: a new tool for protein structure elucidation, *Protein Sci. 2*, 522−531.
40. Zhang, Z., Post, C. B., and Smith, D. L. (1996) Amide hydrogen exchange determined by mass spectrometry: application to rabbit muscle aldolase, *Biochemistry 35*, 779−791.
41. Miranker, A., Robinson, C. V., Radford, S. E., Aplin, R. T., and Dobson, C. M. (1993) Detection of transient protein folding populations by mass spectrometry, *Science 262*, 896−900.
42. Hvidt, A., and Nielsen, S. O. (1966) Hydrogen exchange in proteins, *Adv. Protein Chem. 21*, 287−385.
43. Bai, Y., Milne, J. S., Mayne, L., and Englander, S. W. (1994) Protein stability parameters measured by hydrogen exchange, *Proteins 20*, 4−14.
44. Resing, K. A., and Ahn, N. G. (1998) Deuterium exchange mass spectrometry as a probe of protein kinase activation. Analysis of wild-type and constitutively active mutants of MAP kinase kinase-1, *Biochemistry 37*, 463−475.
45. Engen, J. R., Gmeiner, W. H., Smithgall, T. E., and Smith, D. L. (1999) Hydrogen exchange shows peptide binding stabilizes motions in Hck SH2, *Biochemistry 38*, 8926−8935.
46. Wang, F., Blanchard, J. S., and Tang, X. J. (1997) Hydrogen exchange/electrospray ionization mass spectrometry studies of substrate and inhibitor binding and conformational changes of *Escherichia coli* dihydrodipicolinate reductase, *Biochemistry 36*, 3755−3759.
47. Halgand, F., Dumas, R., Biou, V., Andrieu, J. P., Thomazeau, K., Gagnon, J., Douce, R., and Forest, E. (1999) Characterization of the conformational changes of acetohydroxy acid isomeroreductase induced by the binding of Mg^{2+} ions, NADPH, and a competitive inhibitor, *Biochemistry 38*, 6025−6034.
48. Matagne, A., Jamin, M., Chung, E. W., Robinson, C. V., Radford, S. E., and Dobson, C. M. (2000) Thermal unfolding of an intermediate is associated with non-Arrhenius kinetics in the folding of hen lysozyme, *J. Mol. Biol. 297*, 193−210.
49. Yang, H., and Smith, D. L. (1997) Kinetics of cytochrome *c* folding examined by hydrogen exchange and mass spectrometry, *Biochemistry 36*, 14992−14999.
50. Tsui, V., Garcia, C., Cavagnero, S., Siuzdak, G., Dyson, H. J., and Wright, P. E. (1999) Quench-flow experiments combined with mass spectrometry show apomyoglobin folds through an obligatory intermediate, *Protein Sci. 8*, 45−49.
51. Wang, F., and Tang, X. J. (1996) Conformational heterogeneity and stability of apomyoglobin studied by hydrogen/deuterium exchange and electrospray ionization mass spectrometry, *Biochemistry 35*, 4069−4078.
52. Eyles, S. J., Radford, S. E., Robinson, C. V., and Dobson, C. M. (1994) Kinetic consequences of the removal of a disulfide bridge on the folding of hen lysozyme, *Biochemistry 33*, 13038−13048.
53. Kragelund, B. B., Robinson, C. V., Knudson, J., Dobson, C. M., and Poulsen, F. M. (1995) Folding of a four-helix bundle: studies of acyl-coenzyme A binding protein, *Biochemistry 34*, 7217−7224.

54. Gross, M., Robinson, C. V., Mayhew, M., Hartl, F. U., and Radford, S. E. (1996) Significant hydrogen exchange protection in GroEL-bound DHFR is maintained during iterative rounds of substrate cycling, *Protein Sci. 5*, 2506−2513.
55. Deng, Y., and Smith, D. L. (1999) Rate and equilibrium constants for protein unfolding and refolding determined by hydrogen exchange-mass spectrometry, *Anal. Biochem. 276*, 150−160.
56. Zhang, Z., and Smith, D. L. (1996) Thermal-induced unfolding domains in aldolase identified by amide hydrogen exchange and mass spectrometry, *Protein Sci. 5*, 1282−1289.
57. Bensadoun, A., and Weinstein, D. (1976) Assay of proteins in the presence of interfering materials, *Anal. Biochem. 70*, 241−250.
58. Font, B., Vial, C., Goldschmidt, D., Eichenberger, D., and Gautheron, D. C. (1981) Heart mitochondrial creatine kinase solubilization. Effects of mitochondrial swelling and SH group reagents, *Arch. Biochem. Biophys. 212*, 195−203.
59. Connelly, G. P., Bai, Y., Jeng, M. F., and Englander, S. W. (1993) Isotope effects in peptide group hydrogen exchange, *Proteins 17*, 87−92.
60. Deng, Y., Zhang, Z., and Smith, D. L. (1999) Comparison of continuous and pulsed labeling amide hydrogen exchange/mass spectrometry for studies of protein dynamics, *J. Am. Soc. Mass Spectrom. 10*, 675−684.
61. Bai, Y., Milne, J. S., Mayne, L., and Englander, S. W. (1993) Primary structure effects on peptide group hydrogen exchange, *Proteins 17*, 75−86.
62. Stryer, L. S. (1965) The interaction of a naphthalene dye with apomyoglobin and apohemoglobin. A fluorescent probe of nonpolar binding sites, *J. Mol. Biol. 13*, 482−495.
63. Kiefhaber, T., and Baldwin, R. L. (1996) Hydrogen exchange and the unfolding pathway of ribonuclease A, *Biophys. Chem. 59*, 351−356.
64. Deng, Y., and Smith, D. L. (1999) Hydrogen exchange demonstrates three domains in aldolase unfold sequentially, *J. Mol. Biol. 294*, 247−258.
65. Guijarro, J. I., Jackson, M., Chaffotte, A. F., Delepierre, M., Mantsch, H. H., and Goldberg, M. E. (1995) Protein folding intermediates with rapidly exchangeable amide protons contain authentic hydrogen-bonded secondary structures, *Biochemistry 34*, 2998−3008.
66. Kobashigawa, Y., Demura, M., Koshiba, T., Kumaki, Y., Kuwajima, K., and Nitta, K. (2000) Hydrogen exchange study of canine milk lysozyme: stabilization mechanism of the molten globule, *Proteins 40*, 579−589.
67. Perraut, C., Clottes, E., Leydier, C., Vial, C., and Marcillat, O. (1998) Role of quaternary structure in muscle creatine kinase stability: tryptophan 210 is important for dimer cohesion, *Proteins 32*, 43−51.
68. Mei, G., Di Venere, A., Buganza, M., Vecchini, P., Rosato, N., and Finazzi-Agro', A. (1997) Role of quaternary structure in the stability of dimeric proteins: the case of ascorbate oxidase, *Biochemistry 36*, 10917−10922.
69. Bose, K., and Clark, A. C. (2001) Dimeric procaspase-3 unfolds via a four-state equilibrium process, *Biochemistry 40*, 14236−14242.

BI049965B